

See discussions, stats, and author profiles for this publication at: <https://www.researchgate.net/publication/304665720>

Automatic glaucoma assessment from angio-OCT images

Conference Paper · April 2016

DOI: 10.1109/ISBI.2016.7493242

CITATIONS

0

READS

13

3 authors, including:



Karthik Gopinath

International Institute of Information Technolo...

1 PUBLICATION 0 CITATIONS

SEE PROFILE



Jayanthi Sivaswamy

International Institute of Information Technolo...

89 PUBLICATIONS 862 CITATIONS

SEE PROFILE

Automatic Glaucoma Assessment from Angio-OCT Images

Karthik Gopinath* Jayanthi Sivaswamy* Tarannum Mansoori†

* CVIT, IIT-Hyderabad, India

† Anand eye institute, Hyderabad, India

ABSTRACT

A variety of imaging modalities have been used for developing diagnostic aids for glaucoma assessment. Structural imaging modalities such as colour fundus imaging and optical coherence tomography (OCT) have been investigated for automatically estimating key parameters for glaucoma assessment such as cup to disc diameter ratio and thickness of the retinal nerve fibre layer (RNFL). OCT-based angiography or OCTA is a new modality which provides structural and angiographic information about the retinal layers. We present a method for glaucoma detection using OCTA images. Specifically, the capillary density at various layers and thickness of RNFL are estimated and used to classify a given OCTA volume as glaucomatous or not. RNFL thickness is estimated using polynomial fitting to intensity profiles of OCT slices. The capillary density is estimated from the angioflow images using morphological processing to extract the optic nerve head (ONH) and vessel detection in a region of interest defined around the ONH. A system trained on these two features was evaluated on a dataset of 67 eyes (49 normal and 18 glaucomatous) and found to have a sensitivity of 94.44 % and specificity of 91.67%. This demonstrates the potential of the new modality for glaucoma assessment.

Index Terms— Angio-OCT, RNFL thickness, Glaucoma

1. INTRODUCTION

Glaucoma is a common cause of irreversible blindness globally. Clinically, it is characterized by loss of retinal ganglion cells, neural rim tissue and manifests as an enlargement of the optic cup and peripapillary retinal nerve fiber layer (RNFL) loss. Prevention of glaucoma requires understanding the pathogenesis of the disease and early detection of the disease which in turn depends on the ability to recognize early clinical manifestations. RNFL thickness measurement by OCT is a useful for early diagnosis of glaucoma. The cup enlargement is quantified by cup to disc diameter ratio (CDR) and can be estimated either from colour fundus image or OCT. Some automated methods for computing the CDR have been put forth in [1] and [2].

Spectral domain OCT is widely used in ocular disease detection and algorithms have been proposed for segmenting the layers from OCT images[3][4]. The RNFL thickness is a biomarker for glaucoma [5][6] and hence, OCT scanner-generated reports generally provide the *deviation* of the peripapillary RNFL thickness of a current measurement from normative database across various regions around the ONH.

Clinical research has also aimed at understanding the cause of glaucoma from *vascular health* point of view. Post-mortem studies on eyes have found selective atrophy of radial peripapillary capillaries in the superficial layers [7] in glaucomatous eyes and a correlation between RNFL thickness and capillary volume [8] in normal eyes. Fluroscin angiography conducted on 75 subjects (50 with glaucoma) has also provided evidence for correlation between glaucomatous disc damage and capillary drop out in the surface layers [9].

OCT based angiography (OCTA) is a new imaging modality providing angioflow profiles at various layers of the retina. It is based on a rapid OCT scanning of the eye at the same location in the retina, over a time interval, to look for changes in the scan. All the structures in the retina are static except for the blood flow through vasculature or by movement of the eye itself. Mapping these areas of blood flow is done using the Split-Spectrum Amplitude-Decorrelation Angiography algorithm [10] to derive highly detailed maps of the vasculature in a noninvasive manner as opposed to fluroscin angiography. Specifically, in addition to structural information about the retinal layers, OCTA also provides angioflow (enface or top view) images which capture angiographic information at different layers namely, the superficial capillary plexus, deep capillary plexus, outer retina and choriocapillaris area which aid a detailed study of the capillary network.

We propose a framework for glaucoma assessment from OCTA images. Part of the goal in developing this framework is to gain insights into the correlation between capillary drop out at various layers and RNFL thickness in predicting glaucoma. Hence, the framework is based on the RNFL thickness and capillary density around ONH. The former is estimated from the OCTA slices while the latter is derived from the angioflow (enface) images. The proposed method has been validated against data collected from 49 normal and 18 glaucomatous eyes.

This work was supported by the Dept. of Electronics and Information Technology, Govt. of India under Grant: DeitY/R&D/TDC/13(8)/2013.

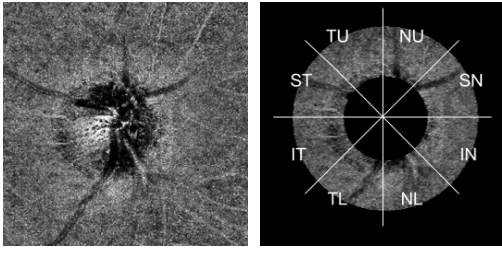


Fig. 1: Choroid Disc Angioflow image (left) and Eight sectors of ROI (right) for a Right Eye.

2. PROPOSED METHOD

The input for the proposed system is an OCTA volume and four angioflow images of the Choroid disc, Nerve head (NH), Radial Peripapillary Capillaries (RPC) and the Vitreous layer. OCTA volume provides structural information about the retinal layers whereas the 2D angioflow images provide information about blood flow in a specific layer. The proposed system comprises of 3 stages: Extraction of region of interest (ROI) centred around OD; Feature extraction, explained in section 2.2 and Classification. The ROI is an annular region around the ONH. The capillary network is extracted using vessel detection and suppression of large vessels from the angioflow images. The RNFL layer thickness is calculated based on the intensity profile (at the slice level) from the OCTA volume. A linear SVM classifier is trained using these information for the classification task.

2.1. Extraction of Region of interest

Among the 4 OCTA angioflow images, the ONH boundary has the best definition and hence is detectable in the choroid disc angioflow image (I_{cen}). A sample choroid disc angioflow image is shown in Fig. 1. The central dark region is the ONH. I_{cen} is used to extract the ROI as follows: The local minima in the image is found using a filter of size 3×3 , following which all small objects are removed; The centroid of the large central dark object is found and a circle fitting operation is used to extract the ONH region; Finally, an annular region of 100 pixels width around the detected ONH is extracted as the desired ROI. The ROI is divided into eight sectors with sector angle equal to 45° (Fig. 1) to identify the Temporal Upper (TU), Temporal Lower (TL), Superior Temporal (ST), Inferior Temporal (IT), Nasal Upper (NU), Nasal Lower (NL), Superior Nasal (SN), Inferior Nasal (IN) regions. The nasal and temporal sectors are mirrored about the vertical for the right and left eyes.

2.2. Feature extraction

For every sector in the ROI, two metrics, namely the capillary density (CD) and RNFL thickness are of interest. The procedure for deriving these metrics is explained next.

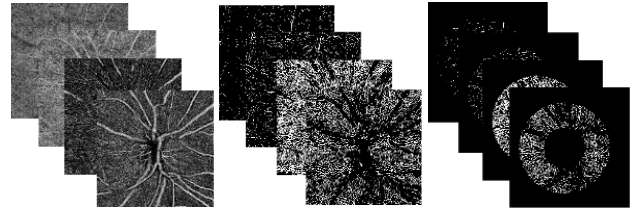


Fig. 2: Estimation of Capillary Density. (a) Angioflow im- (b) Detected capil- (c) Capillaries in the ages. lary network. ROI.

Fig. 2: Estimation of Capillary Density.

2.2.1. Capillary Density estimation

An angioflow image is the input for the CD computation. Non-uniform illumination is a problem seen in these images. This is corrected with a modified quotient based approach [11]. Here, the given degraded retinal image I , is modelled as a multiplicative degradation function L applied to an ungraded/original image I_o . L is assumed to be a slowly varying function and thus estimated from the smoothed version (I_s) of the degraded image as:

$$L(x, y) = \begin{cases} \frac{I_s(x, y)}{l_o} & \text{if } I_s(x, y) < l_o \\ 1 & \text{if } I_s(x, y) \geq l_o \end{cases} \quad (1)$$

where l_o is the desired mean illumination level, chosen to be half the dynamic pixel range of I . Using the above estimate of L , the desired image I_o is found as:

$$I_o(x, y) = \begin{cases} I(x, y) \times \frac{l_o}{I_s(x, y)} & \text{if } I_s(x, y) < l_o \\ I(x, y) & \text{if } I_s(x, y) \geq l_o \end{cases} \quad (2)$$

Next, vessels are detected using the Bar-Combination Of Shifted Filter Responses [12]. Parameters for the Gaussians in the Difference-of-Gaussians filters in [12] were tuned to extract only large vessels. These were suppressed in the angioflow image to retain the capillary network. Fig. 2 (a) and (b) show angioflow images from a sample OCTA and the derived capillary network. The CD for a given angioflow image is found as

$$CD(m) = \frac{N(m)}{A(m)} \quad (3)$$

Here, N is the number of capillary pixels and A is the area of the m^{th} sector with $m = 1, 2, \dots, 8$. CD is computed for each of the 4 angioflow images (per eye), to derive a set of 8-dimensional (8-D) vectors representing the CD at 4 different layers. The capillary loss is inversely proportional to the calculated CD.

2.2.2. RNFL thickness estimation

The RNFL thickness is computed from the slices of the OCTA volume of size $M \times N \times K$. The size of the ONH varies

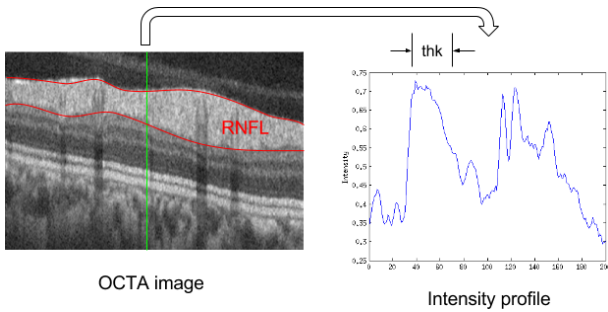


Fig. 3: Estimation of RNFL thickness from intensity profile.

across subjects and as a result the sector area in the ROI is also varies. Hence, we chose to represent the RNFL thickness in a sector by the mean value and not a vector. We propose a computationally efficient method for RNFL layer segmentation. This is based on the analysis of the intensity profiles along the columns of an OCTA slice. Given a $M \times N$ slice, each column is analysed as a M -D intensity profile Fig. 3 shows a sample column (in green) and the corresponding intensity profile. The first major sharp rise in the intensity profile is due to dark to bright transition corresponding to the Inner Limiting Membrane (ILM) boundary. After ILM boundary, a large dip in intensity marks the RNFL boundary. The width of the first major peak in the profile corresponds to the RNFL thickness. We hence locate the first local maxima and fit a second order polynomial to the profile around this peak. The full width at half the maximum value of the first peak is taken as the RNFL thickness.

2.3. Classifier

The input to the classifier is a combination of the CD and RNFL thickness features. The CD values for 8 sectors across 4 angioflow images give rise to a 4×8 CD matrix. The RNFL thickness is a 1×8 vector which is added to the CD matrix to form the final 5×8 matrix. This matrix is converted to a 1×40 feature vector which forms the input to a linear SVM.

3. EXPERIMENTS AND RESULTS

Dataset: OCTA images from an Optovue scanner (spectral domain RTVue - XR 100 OCT (Avanti edition, Optovue, Inc, CA)) were collected from a local hospital. The dataset consists of images of 67 eyes (49 normal and 18 glaucomatous). The data for each eye consisted of a OCTA volume and angioflow images of the choroidal disc, nerve head, RPC and the vitreous layers. The OCTA volume was of size $640 \times 304 \times 304$ while the angioflow images were of size (304×304) . Ground truth for each eye was obtained based on clinical examination by one expert (co-author).

A six-fold validation was done to assess the performance of the system. For each fold of the training set, features were

Table 1: Performance of the proposed system with only RNFL thickness or CD features.

	RNFL alone		CD alone	
	Mean	Std.	Mean	Std.
Sensitivity	0.4444	0.1721	0.8333	0.1826
Specificity	0.8773	0.1370	0.7986	0.1429
Accuracy	0.7601	0.1258	0.8081	0.0971

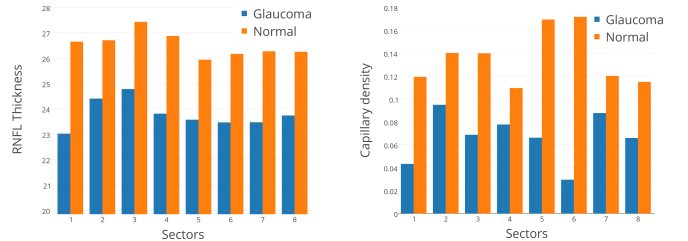


Fig. 4: RNFL thickness (left) and Capillary density (right) variation for a Glaucomatous and a Normal case across sectors. The latter is averaged over 4 angioflow images(layers).

taken from 15 glaucomatous and 40 normal class images. Post training, test samples were given to the learnt model to predict the class. Quantitative evaluation of the method is done by computing sensitivity, specificity and accuracy across the folds. The sensitivity, specificity and accuracy metrics were found using the formulae below. Here, T/FP denote True/False Positive, T/FN denote True/False Negative.

$$Sensitivity = \frac{TP}{TP + FN} \quad Specificity = \frac{TN}{TN + FP}$$

$$Accuracy = \frac{TP + TN}{TP + TN + FP + FN}$$

The RNFL thickness and CD values across the 8 sectors are presented for one Glaucomatous and one normal eye image in Fig 4. Both plots exhibit a common trend in that the values for the glaucomatous eye is lower than that for the normal eye. Based on this trend, we expect the two features to be effective in discriminating between the two classes.

The effect of using either of these features exclusively, on classification was studied. Results are tabulated in Table 1. Classification with just RNFL thickness feature is seen to result in low sensitivity and accuracy values, even though the specificity is better compared to that obtained with exclusively CD features computed from all 4 angioflow images. Thus, it appears that the vascular health information is generally more effective in attaining good glaucoma classification.

Next, we report on an experiment in which both CD and RNFL features were used for classification. Results are shown in Table 2. The relative importance of each angioflow image can be gauged based on the results reported for CD

Table 2: Performance of the proposed system with RNFL and CD features from layers. Best results are in bold font.

	RNFL + Choroidal disc		RNFL + NH		RNFL + RPC		RNFL + Vitreous		RNFL + All layers	
	Mean	Std.	Mean	Std.	Mean	Std.	Mean	Std.	Mean	Std.
Sensitivity	0.7222	0.1361	0.6111	0.2509	0.7778	0.1721	0.7778	0.2722	0.9444	0.1361
Specificity	0.6944	0.1701	0.7755	0.1658	0.8218	0.1891	0.9005	0.1167	0.9167	0.1021
Accuracy	0.7008	0.1257	0.7298	0.1429	0.8081	0.0971	0.8662	0.0745	0.9242	0.0859

from each angioflow individually. The top two results are seen to be obtained for the vitreous and RPC angioflow images. Thus, vascular health information at these top two retinal layers appear to be relatively more important for correct glaucoma assessment. The last column in the Table 2 is the result for the full set of features: CD features from all layers and RNFL thickness. The performance is best for this case with all the metrics being above 90%.

The RNFL estimation in our proposed method uses a simple technique. In order to determine if a finer segmentation method can improve the classification performance, we experimented with a graph-based layer segmentation algorithm [3]. However, this yielded only a marginal improvement. This is because the thickness of the RNFL layer in a sector is represented only by its mean value and thus the proposed method is well equipped for the classification task. Since OCTA is a new modality there is no reported work on glaucoma classification from Angio-OCT images and hence bench marking cannot be done.

4. CONCLUSIONS

Inspired by the clinical significance of capillary loss and nerve fiber thickness, a novel method for automated glaucoma detection study is proposed using images from a new modality. The method relies on a RNFL thickness and capillary density from OCTA data. While the capillary loss alone appears to be relatively better for glaucoma classification, compared to RNFL thickness, it was also found that the best performance with a comprehensive set of features representing the vascular health (CD) and structural (RNFL) information. Since this is a new imaging modality the proposed work represents the first attempt at its utility for glaucoma assessment application. The obtained results are promising and encourage considering further evaluation on a larger dataset.

5. REFERENCES

- [1] Jun Cheng et al., “Superpixel classification based optic disc and optic cup segmentation for glaucoma screening,” *Medical Imaging, IEEE Transactions on*, vol. 32, no. 6, pp. 1019–1032, 2013.
- [2] Gopal Datt Joshi et al., “Optic disk and cup segmentation from monocular color retinal images for glaucoma assessment,” *Medical Imaging, IEEE Transactions on*, vol. 30, no. 6, pp. 1192–1205, 2011.
- [3] Stephanie J Chiu et al., “Automatic segmentation of seven retinal layers in sdopt images congruent with expert manual segmentation,” *Optics express*, vol. 18, no. 18, pp. 19413–19428, 2010.
- [4] Markus A Mayer et al., “Fuzzy c-means clustering for retinal layer segmentation on high resolution oct images,” .
- [5] Delia Bendschneider et al., “Retinal nerve fiber layer thickness in normals measured by spectral domain oct,” *Journal of glaucoma*, vol. 19, no. 7, pp. 475–482, 2010.
- [6] Markus A Mayer et al., “Retinal nerve fiber layer segmentation on fd-oct scans of normal subjects and glaucoma patients,” vol. 1, no. 5, pp. 1358–1383, 2010.
- [7] Abraham L Kornzweig et al., “Selective atrophy of the radial peripapillary capillaries in chronic glaucoma,” *Archives of ophthalmology*, vol. 80, no. 6, pp. 696–702, 1968.
- [8] K Yu Paula et al., “Correlation between the radial peripapillary capillaries and the retinal nerve fibre layer in the normal human retina,” *Experimental eye research*, vol. 129, pp. 83–92, 2014.
- [9] Niklas Plange et al., “Fluorescein filling defects and quantitative morphologic analysis of the optic nerve head in glaucoma,” *Archives of ophthalmology*, vol. 122, no. 2, pp. 195–201, 2004.
- [10] Yali Jia et al., “Split-spectrum amplitude-decorrelation angiography with optical coherence tomography,” *Optics express*, vol. 20, no. 4, pp. 4710–4725, 2012.
- [11] Saurabh Garg et al., “Unsupervised curvature-based retinal vessel segmentation,” in *Biomedical Imaging: From Nano to Macro, 2007. ISBI 2007. 4th IEEE International Symposium on*. IEEE, 2007, pp. 344–347.
- [12] George Azzopardi et al., “Trainable cosfire filters for vessel delineation with application to retinal images,” *Medical image analysis*, vol. 19, no. 1, pp. 46–57, 2015.